Universal mechanism of thermomechanical deformation in metallic glasses

W. Dmowski, Y. Tong, T. Iwashita, Y. Yokoyama, and T. Egami

Phys. Rev. B **91**, 060101 — Published 11 February 2015

DOI: 10.1103/PhysRevB.91.060101

Universal mechanism of thermo-mechanical deformation in metallic glasses

W. Dmowski[1,*], Y. Tong[1], T. Iwashita[2], Y. Yokoyama[3], and T. Egami[1,2,4]

[1]Department of Materials Science and Eng., University of Tennessee, Knoxville, TN 37996

[2]Department of Physics and Astronomy, University of Tennessee, Knoxville, TN 37996

[3]Institute for Materials Research, Tohoku University, Katahira, Sendai 980-8577, Japan

[4]Oak Ridge National Laboratory, Oak Ridge, TN 37831

*corresponding author: wdmowski@utk.edu

Abstract:

We investigated the atomistic structure of metallic glasses subjected to thermo-mechanical creep deformation using high energy x-ray diffraction and molecular dynamics simulation. The experiments were performed *in-situ*, at high temperatures as a time dependent deformation in the elastic regime, and *ex-situ* on samples quenched under stress. We show that all the anisotropic structure functions of the samples undergone thermo-mechanical creep can be scaled into a single curve, regardless of the magnitude of anelastic strain, stress level and the sign of the stress, demonstrating universal behavior and pointing to unique atomistic unit of anelastic deformation. The structural changes due to creep are strongly localized within the second nearest neighbors, involving only a small group of atoms.

Keywords: Bulk metallic glasses, shear transformation zones, X-ray diffraction, creep,

PACS: 61.05.cp, 62.20.Hg, 81.05.K

Metallic glasses are known for their high mechanical strength and are promising as structural materials [1]. However, in spite of extensive research over many years, the atomistic mechanisms of mechanical deformation in metallic glasses remains poorly understood. A major cause of difficulty in determining the mechanism is that at room temperature deformation in metallic glasses is highly localized in narrow shear bands, and any local structural change induced by deformation is wiped out by subsequent heating [2]. On the other hand thermo-mechanical creep deformation, induced when metallic glass is subjected to stress at elevated temperatures approaching the glass transition, is spatially homogeneous and thus easier to study [e.g. 3]. It is known that creep deformation leaves the sample in a structurally anisotropic state because of anelastic deformation resulting in bond-orientational anisotropy [4,5]. In this work we focus on the structural aspects of the thermo-mechanical creep deformation by using high energy x-ray diffraction and we show that when appropriately scaled, the structural anisotropy induced by creep deformation is independent of time and stress, implying that a universal mechanism of creep deformation exists.

In crystalline materials anelastic and plastic deformation is caused by the movement of lattice defects. In glasses, on the other hand, defects cannot be easily and uniquely identified. Phenomenologically the creep is explained in terms of formation and interaction of the shear transformation zones (STZs) [6, 7]. STZ is an important concept used in explaining mechanical deformation and flow of metallic glasses [8, 9, 10,11]. However, experimental determination of the atomistic details of the STZ has been controversial [12, 13, 14,15]. To shed light on this question we examined the structure of bulk metallic glasses subjected to thermo-mechanical creep in the anealstic, recoverable regime using high energy X-ray diffraction. Diffraction

experiments were performed on samples *in-situ* during time dependent deformation at 300 °C, and *ex-situ* at room temperature, after quenching down the samples crept at 300-350 °C. The quenched samples were submitted to compression during creep. The *in-situ* studies were carried out in tension. All the samples retained fully amorphous in structure.

X-ray diffraction measurements were done at the synchrotron beamlines 1-ID at the APS, Argonne National Laboratory, Argonne and WB5 at the DESY, Hamburg. The incident energy was tuned to 100 keV ($\lambda = 0.1254$ Å). The beam size was 0.2×0.2 mm^2 at 1-ID or 0.4×0.4mm^2 at WB5. GE and Perkin Elmer area detectors were used in collecting diffracted X-rays. We used $Zr_{55}Cu_{30}Ni_5Al_{10}$ (the glass transition temperature: $T_g = 434$ °C; yield stress: $\sigma_y = 1820$ MPa at 300K, and 1450 MPa at 300 °C, 1000 MPa at 350 °C, with strain rate 0.0001/s; structure function and pair distribution function of the as-cast sample are shown in supplement [16], Figure S1) metallic glass to examine creep in different conditions as indicated in the figures. Samples were prepared by melt casting into 8 mm diameter rods [17]. Dog-bone shapes, with the central part being 9.6 mm long and 2×0.6 mm^2 cross-section, were cut using EDM and used for the tension experiment. Compression tests were performed on cylindrical rods (2 mm diameter × 4 mm tall). After EDM cuts materials were polished to establish precise dimensions and to remove surface contaminations. Samples were placed in load frames with internal heaters and annealed under stress with inert gas flow. The *ex-situ* deformation was done up to 7 hours at 350 °C under fixed load of 800 MPa, and up to 1000 MPa for fixed time of 1 hour, while the *in-situ* experiment was carried out in tension for 5 hours at 800 MPa/300°C. For each measurement the background due to dark current was subtracted from the data, and then normalized by the incident beam monitor.

The spherical harmonics expansion was performed on the normalized data to determine the anisotropic components of the structure function $S(Q)$ ($Q = 4\pi\sin\theta/\lambda$, where θ is the diffraction angle) and the pair distribution function (PDF), $g(r)$, as described elsewhere [4,18, 19].

$$g(\boldsymbol{r}) = \sum_{\ell,m} g_\ell^m(r) Y_\ell^m\left(\frac{\boldsymbol{r}}{r}\right), \quad S(\boldsymbol{Q}) = \sum_{\ell,m} S_\ell^m(Q) Y_\ell^m\left(\frac{\boldsymbol{Q}}{Q}\right), \tag{1}$$

where $Y_\ell^m(\boldsymbol{r}/r)$ are the spherical harmonics. The anelastic deformation is recoverable; therefore, the sample has a memory of the original state which is stored as structural anisotropy. Indeed the structure of the glass, after high-temperature creep, has the anisotropy with the $l = 2$ symmetry [4], and the next term with $l = 6$ is much smaller [20]. For cylindrical symmetry, as in the present case, only the terms with $m = 0$ are non-zero [18]. In the present work the diffraction data are analyzed using only the elliptical ($l = 2$, $m = 0$) terms of the expansion. It has been shown that for affine deformation the derivative of the isotropic term in the $S(Q)$ or $g(r)$ is proportional to the elliptic component and the proportionality constant is equal to the strain, ε_{aff} [4,19],

$$g_{2,aff}^0(r) = -\varepsilon_{aff}\left(\frac{1}{5}\right)^{1/2}\frac{2(1+\nu)}{3} r\frac{d}{dr} g_0^0(r), \quad S_{2,aff}^0(r) = -\varepsilon_{aff}\left(\frac{1}{5}\right)^{1/2}\frac{2(1+\nu)}{3} Q\frac{d}{dQ} S_0^0(Q), \tag{2}$$

where ν is the Poisson's ratio, and $g_2^0(r)$ and $S_2^0(Q)$ are directly related to each other through the second order spherical Bessel transformation.

Figure 1 (a) shows the data obtained *in-situ* during annealing at 300 °C under the constant stress of 800 MPa, which is below the yield point (~ 1500 MPa at 300 °C). The magnitude of $S_2^0(Q)$ was found to increase with holding time. The anisotropic patterns shown in Figure 1 (a) are typical for creep in metallic glasses and are distinct from pure elastic deformation [19] or residual elastic stresses [21]. The dashed line in Figure 1 (a) corresponds to the $S_2^0(Q)$ expected

for affine elastic deformation, which significantly differs from the experimental result on creep deformation. Similar results were obtained for the samples that underwent thermo-mechanical deformation in compression at 350 °/800 MPa for varying time and fixed time/varying stress, and were quenched under stress to room temperature (Figures S2 and S3 in the supplement section [16]). The intriguing feature of the creep strain in metallic glasses is a strong similarity of all of the patterns regardless of the holding time and the stress level. Figure 1 (b) shows elliptical terms for the *in-situ* creep in tension and *ex-situ* creep in compression scaled by some renormalizing constants. The sign of the data for the compression creep is inverted and the data are shifted in Q to adjust for thermal expansion due to different measurement temperatures. Interestingly, the patterns of $S_2^0(Q)$, corresponding to the creep strain can be scaled very well into the same form factor $S_2^0(Q)$, regardless of duration, stress level and the sign of the stress, as shown in Figure 1 (b) (separate scaling for each measurement set is shown in supplement Figures 4,5, and 6 [16]). The constants used in scaling are not exactly proportional to the holding time but are roughly proportional to the stress level. This scaling behavior clearly confirms that the microscopic mechanism of anelastic creep deformation in metallic glasses is well-defined, common, and the same for different modes of deformation (compression and tension) and stress range, contrary to the crystalline materials where different types of defects can be operational, and relates to the viscoelasticity of a glass [22]. The scaling is weakly affected by temperature because the amount of unrecoverable plastic strain depends strongly on temperature, and it is likely that this affects the scaling behavior slightly. Since $g_2^0(r)$ is related by a simple transformation to $S_2^0(Q)$, the same scaling behavior is observed in real space.

To assess the microscopic mechanism of the creep, we compared the anisotropic component of the PDF, $g_2^0(r)$, against the one expected for affine deformation, $g_{2,aff}^0(r)$, using

eq. 2, which gives direct insight into changes in the atomic structure. Figure 2 (a) shows the elliptical term of the pair distribution function after creep in compression at 800 MPa for 7 h at ~350 °C, overlapped with a scaled *in situ* tension data, together with the first derivative of the isotropic term. The derivative is scaled such that the three plots match at large *r*, so that the scaling constant is proportional to the long range or average internal strain. There is a large difference in the amplitude of $g_2^0(r)$ and $g_{2,aff}^0(r)$ at short distances. This is very typical of $g_2^0(r)$ for anelastic creep deformation in metallic glasses. Figure 2 (b) shows the difference, $g_{2,aff}^0(r) - g_2^0(r)$. This difference describes the extent of the local atomic rearrangement which occurred during the creep to relax the applied stress. The local relaxation creates a local stress which balances the internal long-range stress field because the total stress is zero. It is seen that the anelastic deformation is localized to a small group of atoms within the first and second neighbors, and beyond ~8Å the difference is practically zero within experimental resolution. The supplement also shows data (Figure S7 [16]) for a glass with a different composition.

Molecular dynamics studies were performed on a model of amorphous iron [23] with 16,584 atoms to avoid the chemical composition effects. Initially, the structure of a glass was prepared by an instant quench from a liquid at 1500 K to a glass at 700 K, followed by cooling process at 0. 2 K/ps. After gradual cooling to room temperature, the system was relaxed for 2 ns under NTP ensemble with pressure set to zero and temperature at 300K. Initially, the positions of all atoms were homogeneously displaced with a tensile strain of 1% and the Poisson ratio of 0.33. The deformed structure was then relaxed at 300 K. Because computer generated models are quenched at high rates (~10^{11} K/s) they are unstable and show creep behavior even at room temperature. Such elastic heterogeneity was also observed by other molecular dynamics simulations [24, 25]. After the creep each atom in the structure was examined and three groups

were identified: the atoms which retained their original neighbors, the atoms which lost at least one of its neighbors that moved to the next neighbor shell (bond-breaking), and the atoms which gained at least one new neighbor (bond formation). For each atom in the structure the anisotropic component of the pair distribution function was calculated and then summed up according to the above classifications. As a result three $g_2^0(r)$ were obtained: for atoms without local topological change, atoms which lost a neighbor (B-B; bond breaking), and atoms which gained a new neighbor (B-F; bond formation). In the simulation ~10% of all atoms lost or gained a neighbor. Because atoms that have changed their local topology correspond to the shear deformed groups, we have combined these $g_2^0(r)$ (B-B and B-F) into a group that has experienced local topological change (LTC) as shown in Figure 3 (a). The MD result looks qualitatively similar to the experimental data in Figure 2(a) in spite of the difference in composition and time scale. The PDF for LTC atoms and the PDF expected for affine deformation scale well at large *r* and differ significantly in the first atomic shells. Figure 3 (b) shows the difference, $g_{2,aff}^0(r) - g_2^0(r)$, between the affine and LTC, and the affine and Total (average). Despite the differences in composition and temperature, the result for LTC atoms in Fig. 3 (b) is very similar to that in Fig. 2 (b). The plot shows that the local relaxation, which is represented by the difference between the affine and the measured $g_2^0(r)$, originates mostly from the atoms that changed their local topology, even though they represent only ~10 % of all atoms, and suggests that the mechanism of thermo-mechanical creep is local structural relaxation of the applied stress by cutting or forming the atomic bonds. In particular the bonds are severed in a direction of the applied stress, and new bonds are formed in the perpendicular direction. Such bond-exchange processes produce the bond orientational anisotropy previously proposed to explain the structural change after thermo-mechanical creep [4].

In this work we have demonstrated that the pattern of change in the structure function induced by thermo-mechanical creep is independent of the duration, magnitude and sign of the stress applied during creep, suggesting the presence of a well-defined unique, universal mechanism. The structural changes described by the anisotropic PDF are strongly localized to within the second nearest neighbors, and are characterized by the cutting and forming of atomic bonds. Even though the exact details of the changes in the structure are different for each occurrence of local deformation, statistically they result in the repeatable changes in the anisotropic PDF. These actions of cutting and forming of atomic bonds are similar to the elementary excitations in the liquid state [26] in spite of the vast differences in time-scale and temperature. It is likely that the process of changing the local topology of atomic connectivity by cutting and forming the atomic bonds is the basic process of excitation and structural change, both in the liquid state and in the glassy state. This structural behavior may be related to the basic relaxation mechanism in glasses [27,28]. If the results were to be explained in terms of the STZ, the STZs are strongly localized, and composed of cutting and forming local atomic bonds.

Acknowledgement

This work was supported by the Department of Energy, Office of Science, Basic Energy Sciences, Materials Sciences and Engineering Division. Use of the Advanced Photon Source is supported by the U.S. Department of Energy, Office of Science, under Contract No. DE-AC02-06CH11357. We also acknowledge use of the DESY facility, beamline BW5. We thank J. Okasinski (APS) and J. Bednarcik (DESY) for help with experimental setup.

References:

1. A. L. Greer, *Science* **267,** 1945 (1995).

2 . J. J. Lewandowski and A. L. Greer, *Nature Mater.* **5,** 15 (2006).

3. H. S. Chen, *Rep. Prog. Phys.* **43,** 353 (1980).

4. Y. Suzuki, J. Haimovich and T. Egami, *Phys. Rev. B* **35,** 2162 (1987).

5. A. Concustell, S. Godard-Desmarest, M. A. Carpenter, N. Nishiyama, A. L. Greer, *Scripta Mater.* 64, 1091 (2011).

6. A. S. Argon, *Acta Met.* 27, 47 (1979).

7. A. S. Argon and L.T. Shi, *Acta Metal.* **31,** 499 (1983).

8. C. A. Schuh, T.C. Huffnagel and U. Ramamurty, *Acta Mat.* 55, 4067 (2007).

9. A. L. Greer, Y. Q. Cheng and E. Ma, *Materials Science and Engineering R* **74,** 71 (2013).

10. T. Egami, T. Iwashita and W. Dmowski, *Metals* **3,** 77 (2013).

11. J. S. Harmon, M. D. Demetriou, W. L. Johnson, K. Samwer, *Phys. Rev. Lett*. 99 (2007) 135502.

12. D. Pan, A. Inoue, T. Sakura and M.W. Chen, *PNAS* **105,** 14769 (2008).

13. J. D. Ju, D. Jang, A. Nwankpa and M. Atzmon, *J. Apll. Phys.* **109,** 53522 (2011).

14. I-Ch. Choi, Y. Zhao, Y-J. Kim, B-G. Yoo, J-Y. Suh, U. Ramamurty and J. Jang, *Acta Mater.* **60,** 6862 (2012).

15. J.D. Ju, M. Atzmon, *Acta Mater.,* **74**, 183 (2014).

16. See Supplemental Material at [url] for the Figure

17. Y. Yokoyama, K. Inoue and K. Fukaura, *Mater. Trans.* **43,** 2316 (2002).

18. W. Dmowski and T. Egami, *J. Mater. Res*. **22,** 412 (2007).

19. W. Dmowski, T. Iwashita, C-P. Chuang, J. Almer and T. Egami, *Phys. Rev. Lett.* **105,** 205502 (2012).

20. T. Egami, W. Dmowski, P. Kosmetatos, M. Boord, T. Tomida, E. Oikawa and A. Inoue, *J. Non-Cryst. Solids* **192-193,** 591 (1995).

21. Y. Tong, W. Dmowski, Z. Witczak, C.-P. Chuang and T. Egami, *Acta Mater.* **61,** 1204 (2013).

22. M. Schwabe, D. Bedorf, and K. Samwer, Eur. Phys. J. **E 34**, 91 (2011).

23. V. Levashov, T. Egami, R.S. Aga, J.R. Morris, *Phys. Rev. B* **78,** 064205 (2008).

24. Y. Zhang, N. Mattern, J. Eckert*, Intermetallics,* 30, 154, (2012).

25. J. Ding, Y. Q. Cheng, and E. Ma, *Appl. Phys. Lett.*, 101, 121917 (2012).

26. T. Iwashita, D. M. Nicholson and T. Egami, *Phys. Rev. Lett.* **110,** 205504 (2014).

27. G.P. Johari, M. Goldstein, J. Phys. Chem., **74**, 2034 (1970).

28. H.B. Yu, W.H. Wang, H.Y. Bai, and K. Samwer, Nat. Sci. Rev., 1, 1 (2014), Doi:10.1093/nsr/nwu018.

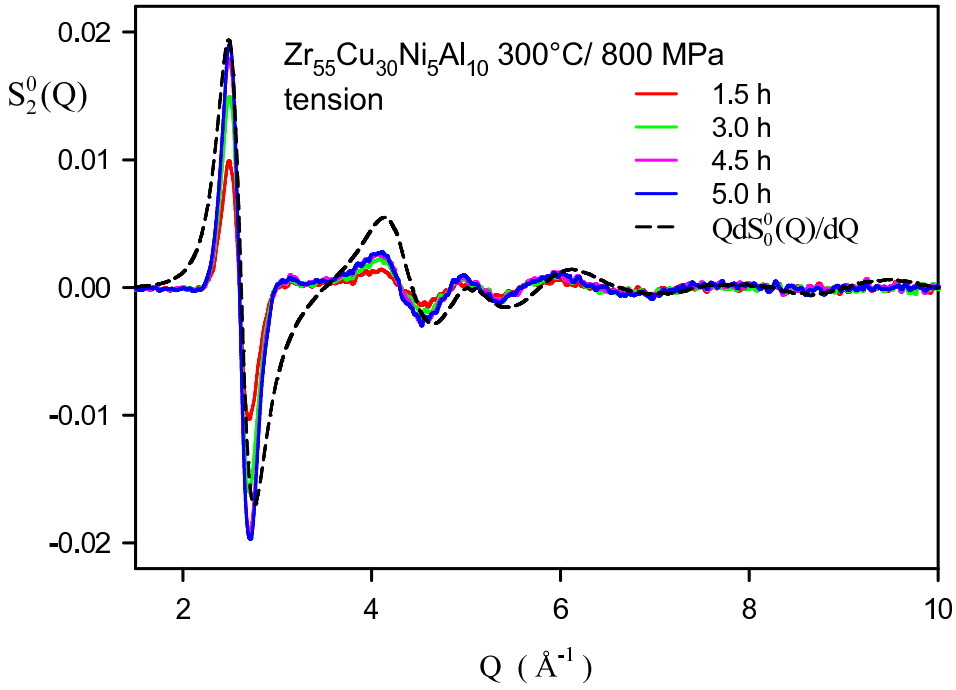

Figure 1a BZR1245 28JAN2015

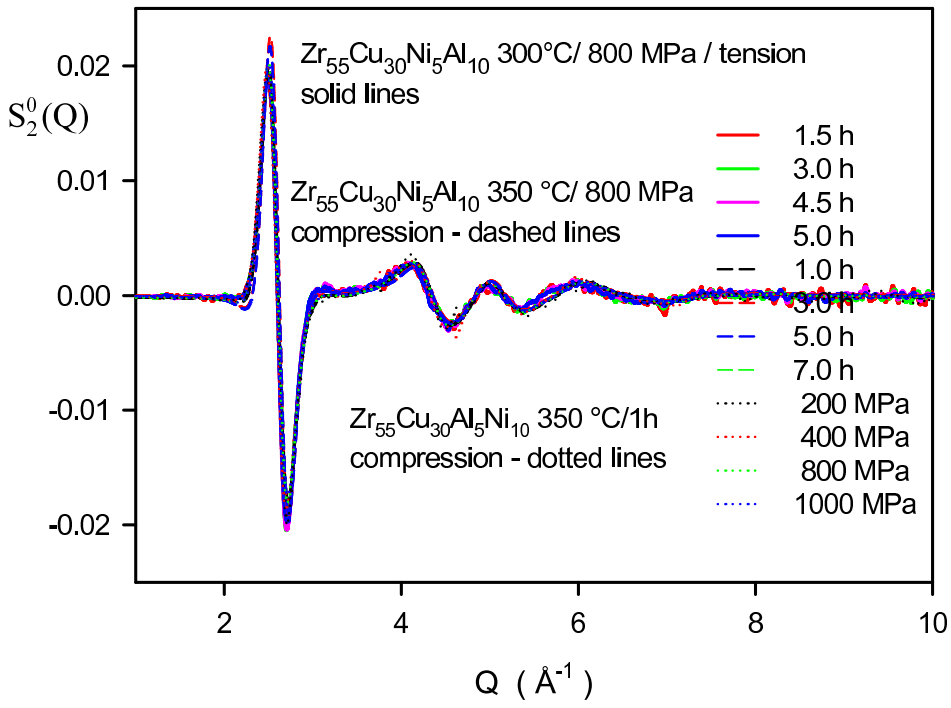

Figure 1b BZR1245 28JAN2015

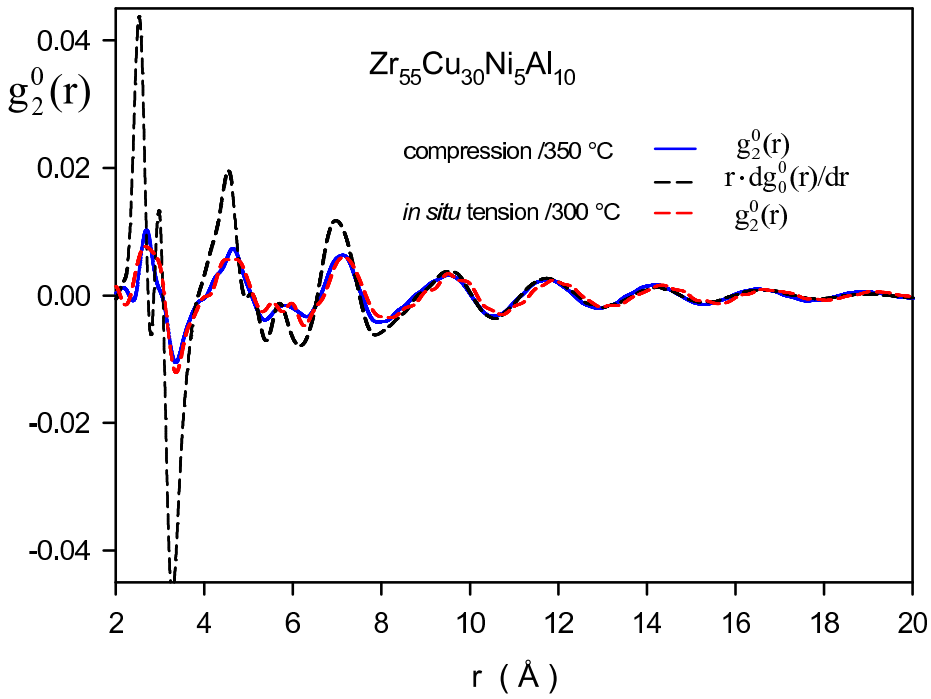

Figure 2a BZR1245 28JAN2015

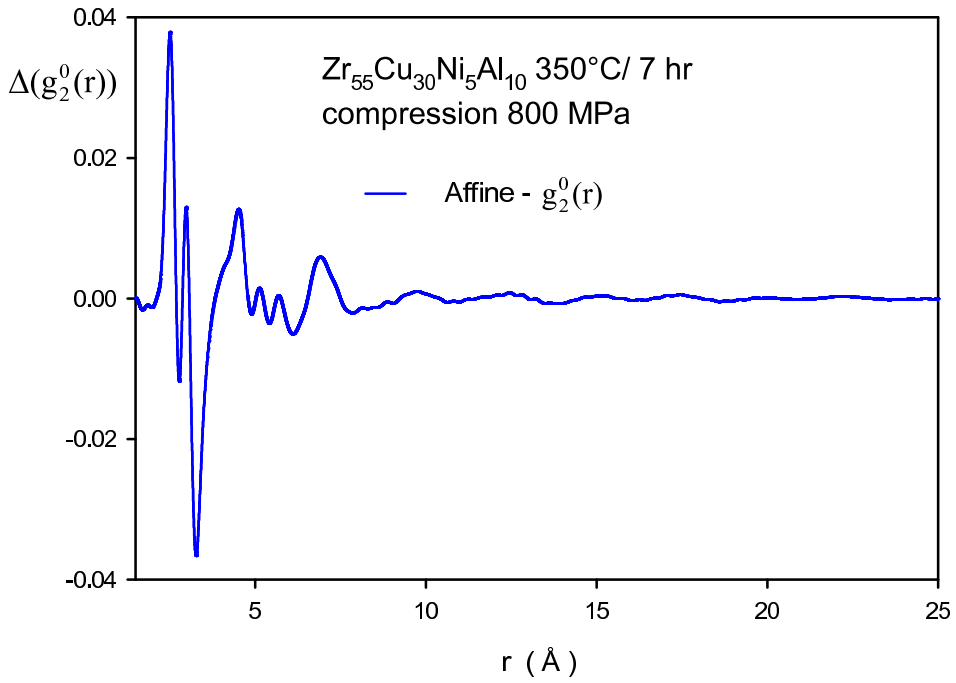

Figure 2b BZR1245 28JAN2015

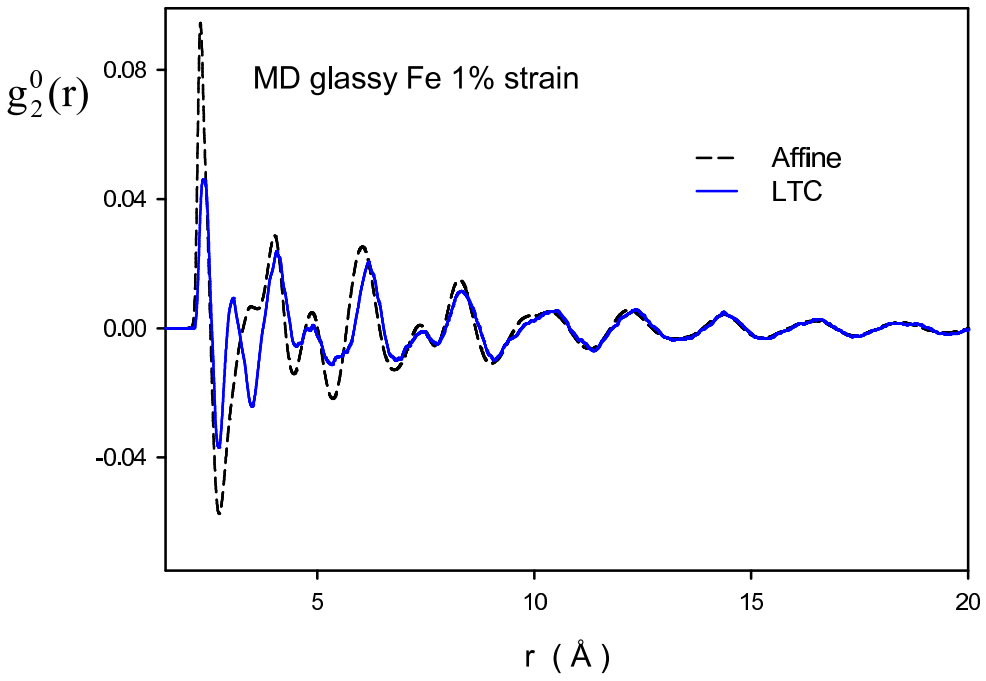

Figure 3a BZR1245 28JAN2015

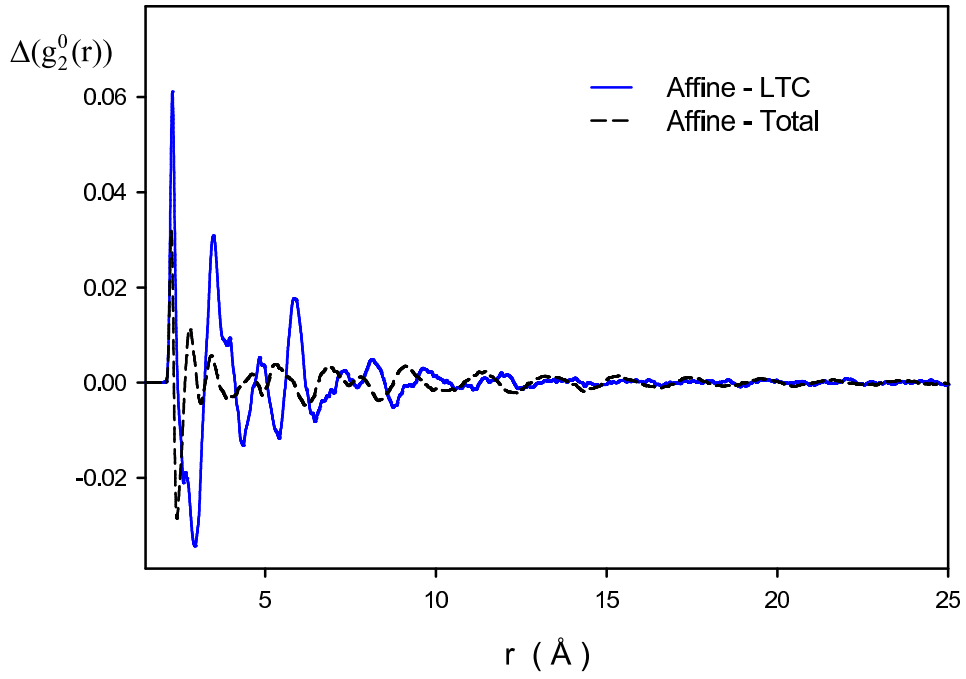

Figure 3b BZR1245 28JAN2015